

Identification of bridge mode shapes using Short Time Frequency Domain Decomposition of the responses measured in a passing vehicle

A. Malekjafarian ^{1,3*}, E.J. OBrien ^{2,3}

¹ Research Assistant, email: abdollah.malekjafarian@ucdconnect.ie

² Professor, email: eugene.obrien@ucd.ie

³ School of Civil, Structural & Environmental Engineering, University College Dublin, Ireland

* Corresponding author. Postal address: School of Civil, Structural & Environmental Engineering, University College Dublin, Newstead, Belfield, Dublin 4, Ireland.

Phone number: +353 1 7163209.

Email address: abdollah.malekjafarian@ucdconnect.ie, a.malekjafarian@gmail.com

Abstract

This paper processes the signals from accelerometers mounted on a vehicle travelling over a bridge. Short Time Frequency Domain Decomposition (STFDD) is used to estimate bridge mode shapes from the dynamic response of the vehicle. In Frequency Domain Decomposition (FDD), several segments are defined on the bridge and the measurement is performed using two instrumented axles. Here, the FDD method is employed in a multi-stage procedure applied to the bridge segments in sequence. A rescaling process is used to construct the global mode shape vector. The performance of the proposed method is validated using numerical case studies. In other indirect bridge identification methods, the road profile may excite the vehicle, making it difficult to detect the bridge modes. This is addressed using two concepts: applying external excitation to the bridge and subtracting signals in the axles of successive trailers towed by the vehicle. The results obtained from the numerical investigation demonstrate that the proposed method can estimate the bridge mode shapes with acceptable accuracy. Sensitivity of the method to added white noise is also investigated.

Key words: Vehicle bridge interaction; Frequency Domain Decomposition; Bridge; Mode shape; Indirect; Identification; SHM; Damage detection; FDD; VBI.

1. Introduction

There is a long history of the use of natural frequency as an indicator of structure and bridge health [1, 2]. Damping ratios [3, 4] and mode shapes [5] have also been used as indicators of health and damage. The dynamic properties of bridges continue today to be a useful evaluation tool in non-destructive damage assessment. The principle is that damage in a bridge leads to some loss of stiffness and consequently to changes in its dynamic properties [6, 7]. In most vibration-based bridge health monitoring techniques, large numbers of sensors are installed on the structure to monitor the dynamic properties. Then, conventional modal testing methods [6] or output-only modal methods [8] can be used to process the measured signals. These approaches, in which sensors are installed directly on the bridge, are known as direct methods [9].

The idea of an indirect approach, in which the natural frequencies of bridge structures are extracted from sensors in a passing vehicle, was first proposed by Yang et al. [10, 11]. In this

approach, a vehicle is instrumented and dynamic properties of the bridge are extracted by processing the dynamic response of the moving vehicle to the bridge. Through interaction between bridge and vehicle, the moving vehicle can be considered as both exciter and receiver. The measured vehicle response needs to include high levels of bridge dynamic response. The feasibility of this method in practice was experimentally confirmed by Lin and Yang [12] by passing an instrumented vehicle over a highway bridge in northern Taiwan. In the case that only bridge frequency is required, the indirect approach showed many advantages in comparison with direct methods in terms of equipment needed, specialist personnel on site, economy, simplicity, efficiency and mobility.

Bu et al. [13] also proposed a bridge condition assessment method based on the dynamic response of a passing vehicle. Yang and Chang [14] applied a pre-processing approach to the measured vehicle response using empirical mode decomposition (EMD) to enhance the resolution of the approach. The effect of several key parameters on the dynamic response of the vehicle passing over the bridge was studied in [15]. It was demonstrated that, unsurprisingly, a larger bridge/vehicle acceleration amplitude ratio results in better accuracy in identifying the bridge frequencies.

McGetrick et al. [16] demonstrated that with a road profile, better accuracy can be obtained at lower vehicle speed. At higher speeds, the road profile's influence on the vehicle vibration dominates the spectrum, hiding the bridge frequency. They showed that changes in bridge damping could be efficiently monitored using the proposed instrumented vehicle. Chang et al. [17] showed that the existence of road surface roughness results in the appearance of vehicle frequencies which cannot be neglected in practice. The feasibility of using an instrumented vehicle to detect the natural frequency and changes in structural damping of a model bridge was investigated by Kim [18, 19] through a scaled laboratory moving vehicle experiment. Yang et al. [20] used two connected vehicles to eliminate the blurring effect of road surface roughness when identifying bridge frequencies.

A novel method for the identification of the damping ratio of a bridge using acceleration measurements from a moving vehicle is proposed in [21]. The appearance of vehicle frequencies in the sensor acceleration spectrum can be a problem, especially when they are close to the bridge first natural frequency [16]. Yang et al. [22] propose some filtering techniques to remove vehicle frequency from the spectrum but these are not always effective. Several types of model test carts were designed and used to improve the experimental accuracy of identifying bridge frequencies from vehicle response in [23]. Keenahan et al. [24] propose a subtraction idea to remove the effect of road profile in the measured response of the vehicle. The obtained results were used to detect the damping changes in the bridge.

Zhang et al. [25] propose a damage index that is based on the squares of the bridge mode shapes, extracted from the acceleration of a passing vehicle applying controlled dynamic forces. The method gives an estimate of the mode shapes. Zhang et al. [26] extended this concept to find the operating deflection shape curvature of the bridges. An optimization method is proposed in [27] to identify bridge frequencies as well as bridge stiffness indirectly using a passing vehicle. Recently, vehicle-based measurement has been extended to construct the mode shapes of bridges theoretically [28]. The instantaneous amplitude history of the bridge component response was obtained using a Hilbert transform of the response measured in the passing vehicle. Although the method worked well when a smooth road profile was used, the accuracy was less in the presence of road roughness. The sensitivity of the method to measurement noise was not considered.

In recent years, several researchers have developed methods to identify the bridge frequency from the acceleration signal in a passing vehicle [10, 11, 22, 23] and to improve the accuracy of the results. In addition, some authors obtained the damping ratio of the bridge using indirect approaches [21, 24], but very few [28] have obtained mode shapes of the bridge indirectly. Estimation of bridge mode shape is very important in a dynamic investigation of a bridge. For instance, there are discontinuities at the damage points in the mode shapes of a damaged bridge, including slope discontinuities at cracks [29, 30]. Furthermore, the bridge mode shape can be used as an important tool in model updating of a bridge [31].

In this paper a novel Short Time Frequency Domain Decomposition (STFDD), using multi-stage measurements, is proposed to obtain bridge mode shape indirectly from accelerations in two connected passing axles. The proposed method is based on the Frequency Domain Decomposition (FDD) method that is an output-only modal testing method. This was first proposed by Brincker et al. [32] to obtain modal parameters of a structure from direct measurements. The proposed method involves two main parts. In the first part, several segments are defined in the bridge and then a multi-stage measurement procedure is done based on the defined segments. The FDD method is applied to the time history acceleration responses from the two following axles in each stage. As a result, local mode shape elements are estimated in each stage in the first part of the method. In the second part, a correction procedure is performed to construct the global mode shape vectors of the bridge from the local estimated mode shape elements.

Numerical case studies are investigated using Finite Element (FE) models of vehicle bridge interaction (VBI) to validate the effectiveness and performance of the proposed method. As noted by many authors [16, 17, 20] the presence of road roughness causes the dominance of vehicle frequencies. Therefore, in the present study, two concepts are tested to address this problem: (a) excitation of the bridge by traffic other than the test vehicle and (b) subtraction of signals measured on following axles. The simulations confirm the capability of the proposed method to identify the mode shapes of a bridge using signals from passing vehicles. Only one accelerometer is assumed on each of the two axles so the proposed method is more efficient than traditional modal testing methods, which usually require the installation of several sensors on the structure.

2. Finite Element modelling of vehicle bridge interaction

In recent years, much research has been carried out on the modelling of vehicle bridge interaction (VBI) [33-36]. González et al. [37] carry out a comprehensive review of coupled and uncoupled VBI models in the literature. A Finite Element (FE) VBI model similar to that used by Keenahan [24] is used here for the numerical investigation of the proposed method. In this model, VBI is modelled as a coupled system in which the solution is calculated at each time step. The vehicle and bridge models and the iterative VBI procedure employed in this paper are set out in the following subsections.

2.1 Vehicle model

The two-quarter-car model shown in Fig. 1 illustrates many of the important characteristics of VBI [38]. This is used here to represent a 2-axle vehicle and, not connecting quarter-cars is a deliberate simplification. Each quarter-car has two independent degrees of freedom corresponding to the translational displacements of body bounce, y_s and axle hop, y_u . The vehicle body and axle

component masses are represented by m_s and m_u (sprung and unsprung). The axle mass connects to the road surface via a spring with linear stiffness k_t which represents the tyre. The equations of motion of the vehicle model are obtained by imposing equilibrium of all forces and moments acting on the masses and expressing them in terms of the degrees of freedom:

$$M_v \ddot{y}_v + C_v \dot{y}_v + K_v y_v = f_{int} \quad (1)$$

where M_v , C_v and K_v are the respective mass, damping and stiffness matrices of the vehicle and \ddot{y}_v , \dot{y}_v and y_v are the respective vectors of nodal acceleration, velocity and displacement. f_{int} is the time-varying dynamic interaction force vector applied to the vehicle degrees of freedom.

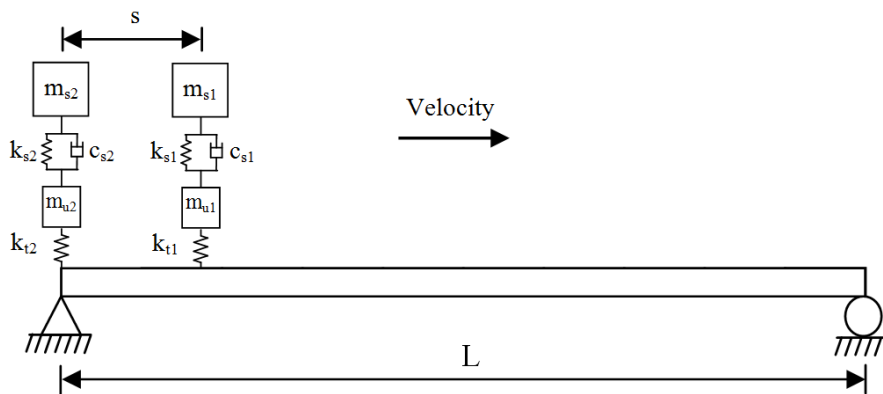


Figure 1: Two following quarter-cars travelling over a bridge.

2.2 Bridge model

A simply supported beam of total span length L is modelled using the FE method to represent the bridge (Fig. 1). The model consists of discretised beam elements with 4 degrees of freedom (2 per node) which have constant mass per unit length, m , modulus of elasticity E and second moment of area J .

The response of the beam model to a series of moving time-varying forces is given by the system of equations:

$$M_b \ddot{y}_b + C_b \dot{y}_b + K_b y_b = f_{int} \quad (2)$$

where M_b , C_b and K_b are global mass, damping and stiffness matrices of the beam model, respectively and \ddot{y}_b , \dot{y}_b and y_b are the vectors of nodal bridge accelerations, velocities and displacements, respectively.

The damping ratio of the bridge, ξ , is considered to be low. Although complex damping mechanisms may be present in the structure, viscous damping is typically assumed for bridge structures and is deemed to be sufficient to reproduce the bridge response accurately. Therefore, Rayleigh damping is adopted here to model viscous damping and is given by:

$$C_b = \alpha M_b + \beta K_b \quad (3)$$

where α and β are constants. The damping ξ is assumed to be the same for all modes and α and β are obtained from $\alpha = 2\xi\omega_1\omega_2/(\omega_1 + \omega_2)$ and $\beta = 2\xi/(\omega_1 + \omega_2)$ where ω_1 and ω_2 are the first two natural frequencies of the bridge [39].

2.3 Coupling of the VBI system

The dynamic interaction between the vehicle and the bridge is implemented in MATLAB. The vehicle and the bridge are coupled at the tyre contact points via the interaction force vector. Combining equations (1) and (2), the coupled equation of motion is formed as:

$$M_g \ddot{u} + C_g \dot{u} + K_g u = F \quad (4)$$

where M_g and C_g are the combined system mass and damping matrices, respectively, K_g is the coupled time-varying system stiffness matrix and F is the system force vector. The vector, $u = \{y_v, y_b\}^T$, is the displacement vector of the system. The equations for the coupled system are solved using the Wilson-Theta integration scheme [40]. The optimal value of the parameter $\theta = 1.420815$ is used for unconditional stability in the integration scheme. The initial condition of the solution is considered to be zero displacement, velocity and acceleration in all simulations.

3. Theory of Short Time Frequency Domain Decomposition method

In this section, the theory of estimation of the bridge mode shapes from the vehicle response using the proposed new method is described. The method contains two fundamental elements; first, applying the FDD method to the measured response of two following vehicles in several stages and second, correction of the estimated local mode shapes in each stage using a rescaling procedure. In order to introduce the method, a short theoretical background of the FDD method is first presented.

3.1 Theoretical background to the FDD method

FDD is an output-only modal analysis method in the frequency domain, first proposed by Brincker et al. [32]. This approach uses the fact that, in a lightly damped structure, modes can be estimated from the spectral densities calculated under a white noise input. In order to obtain the natural frequencies and mode shapes, the power spectral density matrix of the response for each frequency is decomposed by applying Singular Value Decomposition (SVD) to the matrix [41]:

$$\hat{G}_{yy}(\omega_i) = [U]_i [\Sigma]_i [U]_i^H \quad (5)$$

where $[U]_i = [\{u\}_{i1}, \{u\}_{i2}, \dots, \{u\}_{im}]$ is the unitary matrix including the singular vectors $\{u\}_{ik}$ and $[\Sigma]_i$ is a diagonal matrix including singular values σ_{ik} . The superscript "H" indicates the complex conjugate of the matrix and j is equal to $\sqrt{-1}$. If singular values obtained from outputs of the structure are plotted in an SVD diagram, dominant peaks are natural frequencies of the structure and the corresponding singular vectors are mode shapes [25]. More details of the FDD method are provided in the literature [32, 41].

3.2 STFDD method

Many studies have been reported in the literature that use measured accelerations in a passing vehicle for identification of bridge fundamental frequency and damping ratio [10, 11, 22-24, 26]. The measured signal from the vehicle consists of both the bridge response (indirectly) and the vehicle response. Therefore, the fundamental frequency of the bridge and the vehicle frequency are both observable in the fast Fourier transform (FFT) spectrum of the vehicle response. The STFDD method is based on this fact that, if the FDD method is applied to the measured signals from sensors installed on the two following axles in discrete short time periods, the system mode shape can be obtained from a multi-stage procedure. In this paper, the system mode shape is taken as an approximation of the bridge mode shape.

The bridge is divided into a number of segments, each equal in length to the axle spacing. In this example, the axle spacing is, $s=L/5$ and the bridge is divided into five segments, as illustrated in Fig. 2. Four periods (stages) of measurement (Fig. 2) are defined using the five segments of the bridge. The initial locations of the quarter-cars in each stage are shown dotted and the final locations with solid lines.

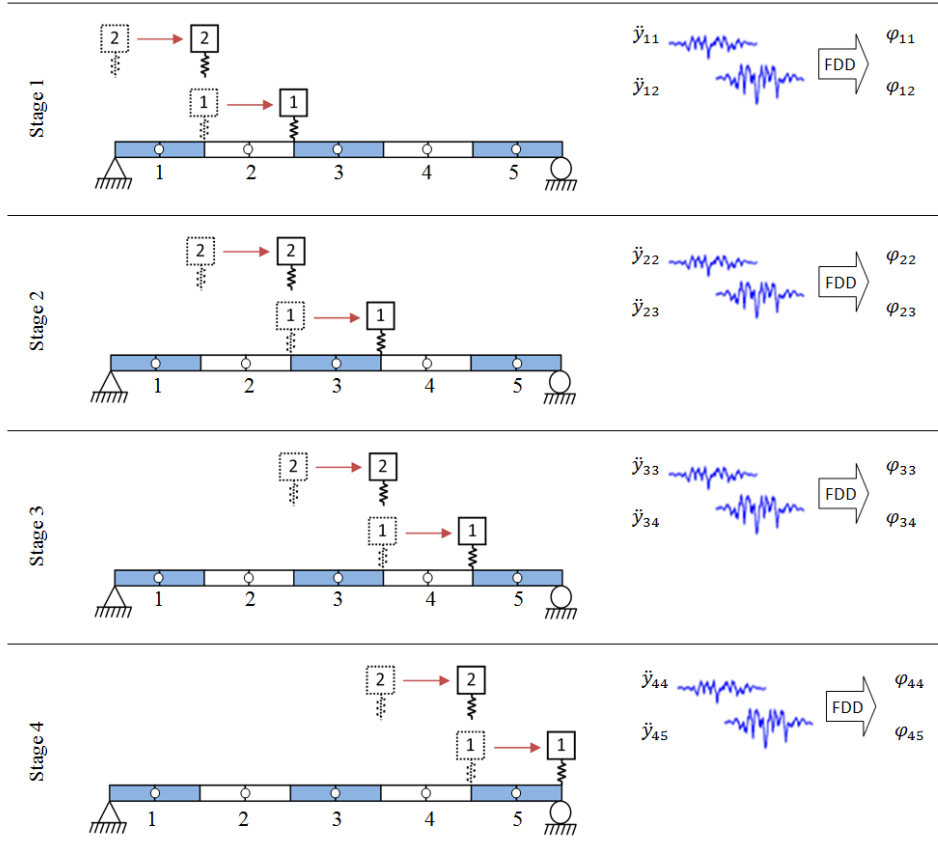


Figure 2: Measurement stages in a 5-segments example.

Two short signals are measured in each stage that are assembled in a matrix:

$$\ddot{Y}_j = \begin{bmatrix} \ddot{y}_{j,j} \\ \ddot{y}_{j,j+1} \end{bmatrix} \quad j=1:4 \quad (6)$$

where $\ddot{y}_{j,j+1}$ and $\ddot{y}_{j,j}$ are the short acceleration response vectors that are measured from axle 1 and axle 2, respectively where the first index indicates the stage number and the second indicates the segment number that the response corresponds to. Therefore \ddot{Y}_j is the response matrix obtained from each stage. The outputs of the measurement procedure in this case are four matrices of data, each including two discrete signals.

In order to estimate the mode shape vector for each stage, the FDD method is applied to the measured data \ddot{Y}_j from each stage. Hence the singular value diagram can be plotted and the natural frequency and two-element vector describing the mode shape can be obtained for each stage as shown in the right hand side of Fig. 2. In this example, four 2-element vectors of mode shape are obtained at four different locations which are called local mode shape vectors $\{\varphi_{j,j}, \varphi_{j,j+1}\}^T$. To estimate the global mode shape vector, a relationship between the local mode shape vectors from the different stages must be established. For this purpose, a progressive rescaling procedure is developed.

The basis of the proposed STFDD method is that the measured signal from each segment of the bridge represents the dynamic behaviour of the bridge for that segment. The first and second elements of the global mode shape vector which are for the first and second segments respectively, are obtained from the first stage:

$$\Phi_1 = \varphi_{11} \quad (7)$$

$$\Phi_2 = \varphi_{12} \quad (8)$$

where Φ_1 and Φ_2 are the global mode shape elements corresponding to the mid-points of the first and the second segments of the bridge. As the signals from Stages 1 and 2 are not measured at the same time, φ_{23} must be rescaled to find the global mode shape of segment 3. The correction ratio is defined based on the local mode shape elements obtained for the common segment in Stages 1 and 2 which are φ_{22} and φ_{12} (or Φ_2). Therefore, the next element of the global mode shape vector Φ_3 is obtained using:

$$\Phi_3 = \varphi_{23} \frac{\Phi_2}{\varphi_{22}} \quad (9)$$

By applying a similar correction procedure, the other elements of the global mode shape vector are obtained, i.e.:

$$\Phi_{j+1} = \varphi_{j,j+1} \frac{\Phi_j}{\varphi_{j,j}} \quad j=2:4 \quad (10)$$

where Φ_{j+1} is the global mode shape element corresponding to the $(j+1)^{th}$ segment which is obtained from the j^{th} stage. The location of the global mode shape elements obtained from the method for each segment is considered to be at the mid-point of that segment.

It should be noted that more mode shape data might be anticipated by considering more bridge segments. However, in increasing the number of segments, the quantities of the measured data for

each segment are decreased which reduces the accuracy of the FDD identification process. Consequently, a compromise number of segments must be chosen for a successful identification procedure.

Although the speed of the vehicle is assumed to be constant in this method, but it is not necessary to keep the speed constant during the implementation. The important thing is that the operator must know which part of the signal is measured in which segment; then it is possible to extract the local mode shapes from the signals, even with variable speed. However, for less complexity and a better result, it is recommended to keep the vehicle speed as constant as possible.

3.3 Example of two quarter-cars on a smooth profile

The STFDD method is tested via numerical simulation using the VBI model described in Section 2. The bridge is modelled using the FE method as a simply-supported beam with the properties given in Table 1. The first three natural frequencies of the bridge are given in Table 2 where it can be seen that the fundamental frequency is 5.65 Hz. The bridge is divided into ten equal segments as shown in Fig. 3.

Table 1. Properties of the bridge.

Properties	Unit	Symbol	value
Length	m	L	15
Mass per unit	kg/m	m	28125
Modulus of elasticity	MPa	E	35000
Second moment of area	m ⁴	J	0.5273

Table 2. First three natural frequencies of the bridge.

Mode No.	1	2	3
Natural frequency (Hz)	5.65	22.62	50.89

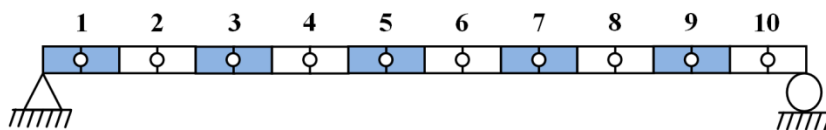


Figure 3: Bridge segments.

As before, the mid-point of each segment is considered to be the location of the global mode shape element obtained for that segment. Therefore, the mode shape vector obtained from the STFDD method will have ten elements corresponding to the ten points shown in the figure. As described in Section 3.2, two following quarter-cars are modelled passing over this bridge (see Fig. 1) with the properties listed in Table 3. The body bounce frequency of both quarter-cars are the same and equal to 12.48 Hz. As explained in Section 3.2, nine stages are considered for the ten segments.

Table 3. Properties of the quarter-cars.

Properties	Unit	Symbol	Value
Body mass	kg	m_s	9300
Axle mass	kg	m_u	350
Suspension stiffness	N/m	k_s	4×10^5
Suspension damping	Ns/m	c_s	10×10^3
Tyre stiffness	N/m	k_t	1.75×10^6
Body bounce frequency	Hz	ω_b	0.94
Axle hop frequency	Hz	ω_a	12.48

The simulation is carried out using the VBI system outlined in Section 2 at the rather slow vehicle velocity of 2 m/s. The time histories of acceleration responses from the two following axles are calculated using a time interval, $dt = 0.001$ s. The FDD method is applied to the nine short time responses of the following axles. The obtained SVD diagrams from the nine stages of the STFDD method are shown in Fig. 4. As the road profile is smooth, vehicle frequencies are not strongly excited and two peaks are clear in all of the SVD diagrams corresponding to the first two natural frequencies of the bridge. As mentioned in Section 3.1, the singular vectors corresponding to these singular values obtained from the peaks of the SVD diagrams, define the local mode shape of each mode in each segment. By applying the rescaling process of the STFDD method to the local mode shapes obtained from the nine stages, the first two global mode shapes of the bridge are obtained and illustrated in Fig. 5. The Modal Assurance Criterion (MAC), defined in Eq. 11, is used to compare the calculated mode shapes to the exact shapes obtained from the FE method:

$$MAC = \frac{|\Phi_{STFDD}^t \Phi_{FE}|^2}{|\Phi_{STFDD}^t \Phi_{STFDD}| |\Phi_{FE}^t \Phi_{FE}|} \quad (11)$$

where Φ_{STFDD} is the global mode shape obtained from the STFDD method and Φ_{FE} is the exact shape obtained from FE method and "t" defines transpose of the matrix. Excellent agreement is found in this case.

4. Effect of road profile

Previous studies [17, 10, 13 and 15] have indicated that estimation of bridge frequency from the vehicle response is difficult in the presence of a road profile. In most cases, although the bridge frequency may be detectable in the spectrum of vehicle response, the vehicle frequencies are dominant.

Yang et al. addressed this challenge in [15] by investigating the effect of several key parameters on the dynamic response of the vehicle passing over the bridge and concluded that, with high vehicle/bridge acceleration amplitude ratios, the probability of successfully identifying the bridge frequency is less. In addition, it was demonstrated in [22] that a larger volume of existing traffic tends to make the bridge frequency more visible. Generally, this solution seems to be practical, especially for longer spans where additional vehicles on the bridge are more likely. Bridge frequency is more visible in the measured response of the passing vehicle when ongoing traffic is modelled in the simulation. However, this is not a good assumption for short-span bridges where the probability of multiple vehicles being present simultaneously on the bridge is small.

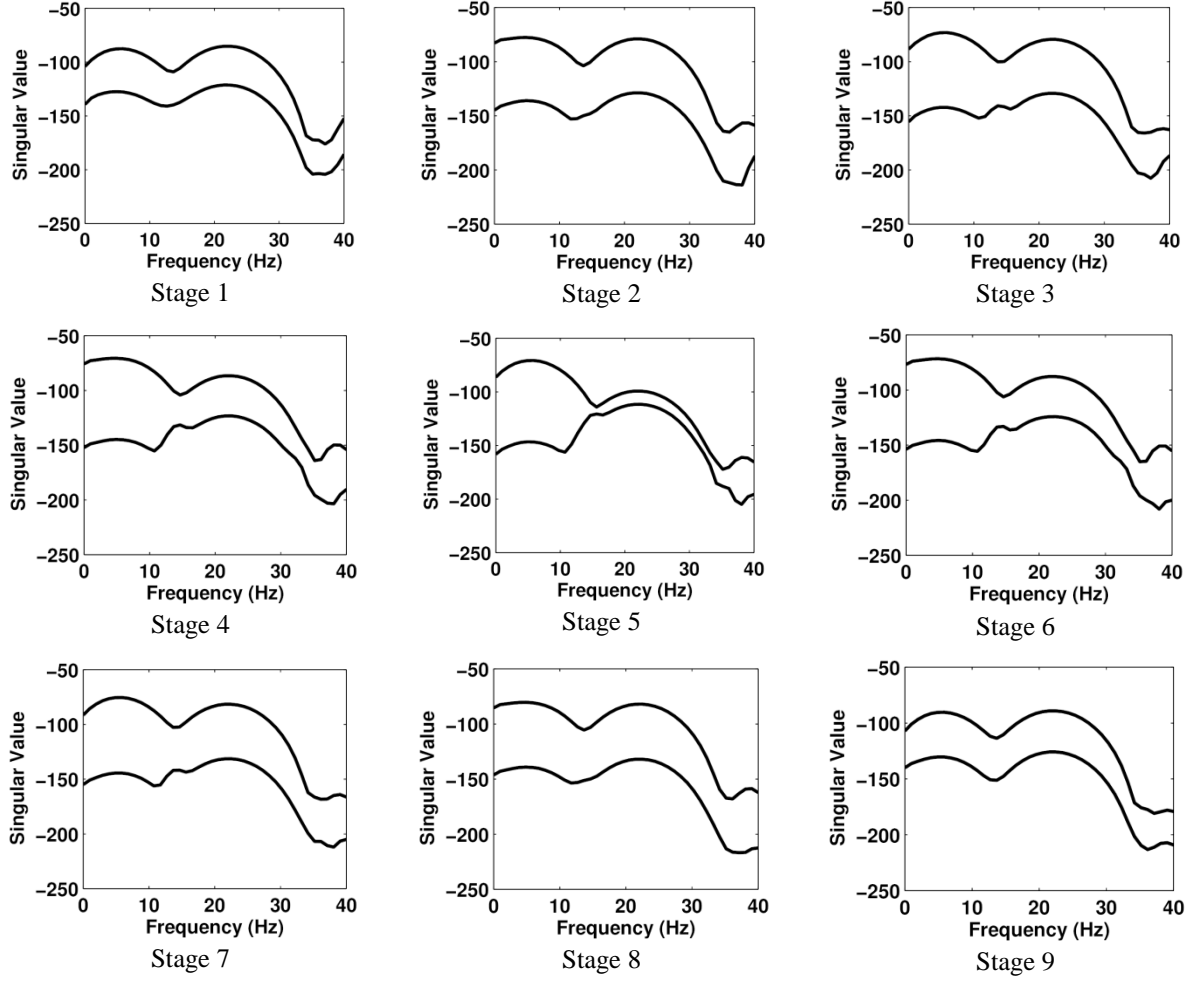


Figure 4: SVD diagrams obtained from nine stages.

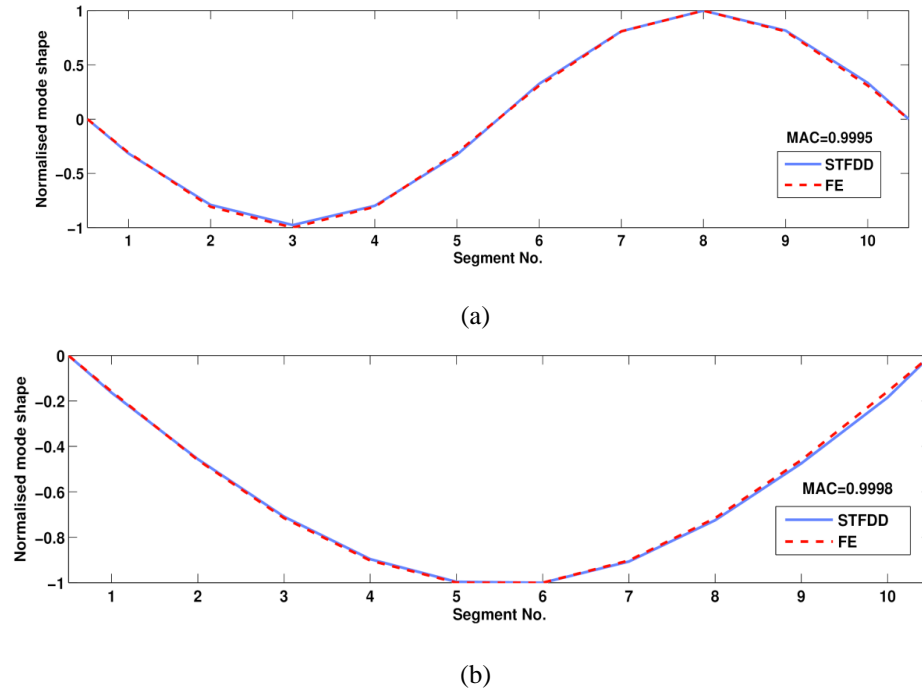


Figure 5: The first two mode shapes of the bridge. (a) First mode shape, (b) Second mode shape.

Recently, Yang et al. [20] and Keenahan et al. [24] proposed the idea of subtraction of the responses to improve the results in the presence of profile. Yang et al. [20] use two connected axles passing over the bridge. It is shown that subtracting the Fourier transform of the two responses gives a residual spectrum in which the bridge frequency is much more clear. However, the method is shown to have some limitations. Keenahan et al. [24] propose the idea of subtracting the measured acceleration responses of two following axles travelling over a bridge. It is demonstrated that the effect of road profile is substantially removed from the residual acceleration response provided the two axles have the same properties.

Both methods of dealing with the road profile are used in this numerical investigation. In the proposed STFDD method, two axle responses are needed to estimate the mode shape values in each stage. Therefore, to implement the concept of subtraction, three following axles are necessary at each stage (see Fig. 6). Four response difference matrices are obtained from the five stages:

$$\ddot{x}_j = \begin{bmatrix} \ddot{x}_{j,j-1} \\ \ddot{x}_{j,j} \end{bmatrix} = \begin{bmatrix} \ddot{y}_{j,j-1} - \ddot{y}_{j-1,j-1} \\ \ddot{y}_{j,j} - \ddot{y}_{j-1,j} \end{bmatrix} \quad j=2:5 \quad (12)$$

where $\ddot{x}_{j,j-1}$ is the difference response obtained in stage j (first index) for segment $j-1$ (second index). The same process of STFDD and the rescaling procedure explained in Section 3.2 is used to obtain the global mode shape vector from the response differences.

	Model	Measured response		
		Axle 3	Axle 2	Axle 1
Stage 1		-	\ddot{y}_{11}	\ddot{y}_{12}
Stage 2		\ddot{y}_{21}	\ddot{y}_{22}	\ddot{y}_{23}
Stage 3		\ddot{y}_{32}	\ddot{y}_{33}	\ddot{y}_{34}
Stage 4		\ddot{y}_{43}	\ddot{y}_{44}	\ddot{y}_{45}
Stage 5		\ddot{y}_{54}	\ddot{y}_{55}	-

Figure 6: Subtraction of measured responses in the presence of a road profile.

4.1 Example of two following quarter-cars crossing a bridge with a Class A profile in the presence of other traffic

The same bridge as for Section 3.3 is now considered, except that a road profile is added. The irregularities of this profile are randomly generated according to the ISO standard [42] for a road class 'A' (very good) profile, as expected in a well maintained highway.

To demonstrate the advantage of an external source of excitation (such as other traffic), a random force which is almost equal to the interaction force of an axle with weight of 4 tonnes is applied to all parts of the bridge. To further improve the quantity of the measured data, the speed of the vehicle is reduced to 1 m/s.

This time, the bridge is divided into six equal segments. The STFDD is applied to the short acceleration signals. As an example, the SVD diagram for Stage 3 is shown in Fig. 7. Although the vehicle frequency is dominant in this SVD diagram, a peak around 5.65 Hz is also visible. However no detectable peak is observed for the second mode of the bridge (around 22.62 Hz) so the second mode shape is not detectable. The first mode shape is shown in Fig. 8 and is less close to the exact shape than before (MAC = 0.9975).

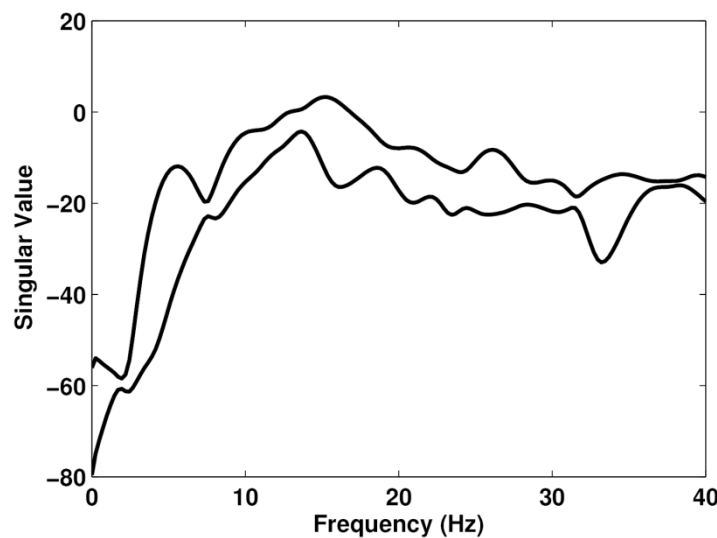


Figure 7: The SVD diagram obtained from Stage 3 when a Class A profile is present.

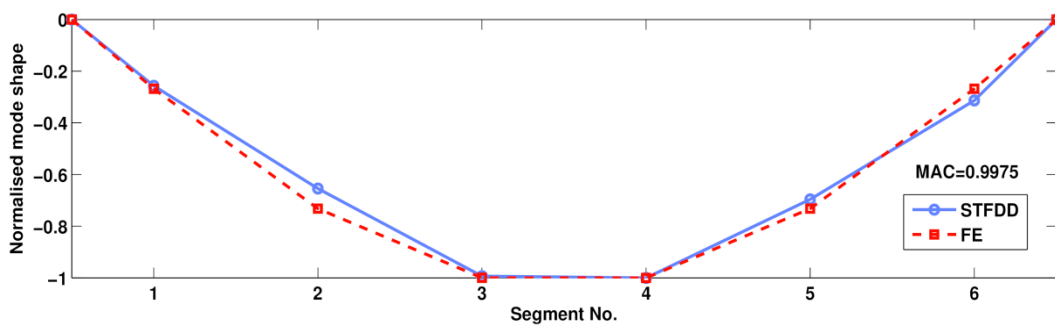


Figure 8: The first mode shape when a Class A profile is present.

While the proposed method is capable of obtaining the bridge fundamental mode shape in the presence of road roughness, it was found to be sensitive to some parameters: (a) the resolution of the measured accelerations which is related to the number of segments and the speed of the vehicle (it works better at lower speed and for longer segments) (b) the closeness of the bridge frequency to a vehicle frequency (closer makes it harder to distinguish the bridge frequency).

As noise is a feature of all measurements, it is necessary to assess the proposed method in the presence of measurement noise. Previous studies [25] have shown that the estimation of bridge dynamic properties from a passing vehicle is not significantly sensitive to noise, since the responses are measured at the same location as the excitation. White noise is added to the calculated vehicle responses to simulate noise-polluted measurements using Eq. 13:

$$w = w_{calc} + E_P N_{noise} \sigma(w_{calc}) \quad (13)$$

where w is the polluted acceleration, E_P is the noise level, N_{noise} is a standard normal distribution vector with zero mean value and unit standard deviation, w_{calc} is the calculated displacement, and $\sigma(w_{calc})$ is its standard deviation. The STFDD method is repeated for different levels of noise and the global mode shape vector is obtained for each level. Fig. 9 shows that the STFDD method, when external excitation is present, can extract the bridge mode shape with acceptable accuracy in the presence of noise up to about 10 %. For noise levels of 5%, 10% and 15%, the MAC values are 0.9982, 0.9974 and 0.9893 respectively.

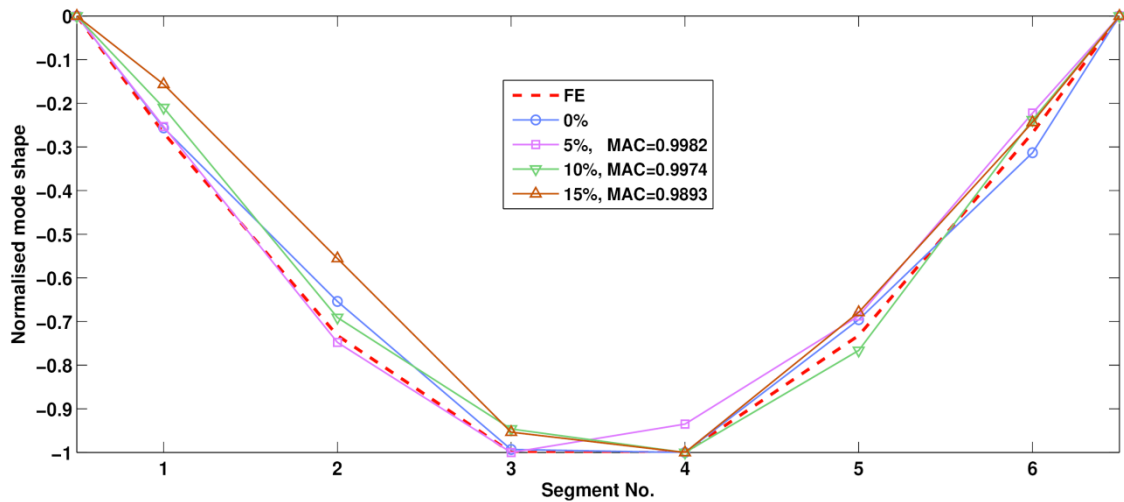


Figure 9: Comparison of the first mode shape vectors for different levels of noise when a Class A profile is present.

4.2 Three following quarter-cars on a bridge with Class A profile

In short span bridge, other traffic may not always be present to provide a source of external excitation. When other traffic is absent, subtracting acceleration responses in following axles is an alternative way to remove the effect of a road profile. To demonstrate the effectiveness of subtraction, three following quarter-cars are simulated travelling over the same bridge as before at a speed of 1 m/s. The bridge is divided into six segments on this occasion. As explained previously, the first signal is the difference in the responses of axles 1 and 2 while the second is the difference

in responses of axles 2 and 3. As an example, the SVD diagram for the third stage is shown in Fig. 10. The quality of the diagram is clearly improved in contrast to what was obtained in Section 4.1. This time, a dominant peak appears around the bridge natural frequency. The peak corresponding to the second mode of the bridge is also clearly detectable in this case. The first two global mode shapes are shown in Fig. 11. The first mode shape is found with good accuracy while the second exhibits some deviation from the exact shape. As the negative effect of road roughness has been removed from the signal in this section, the results show better accuracy in comparison with those of section 4.1

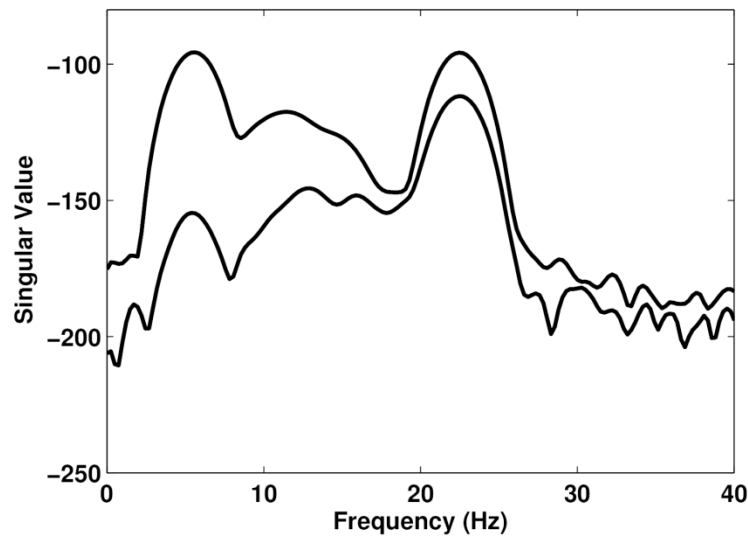
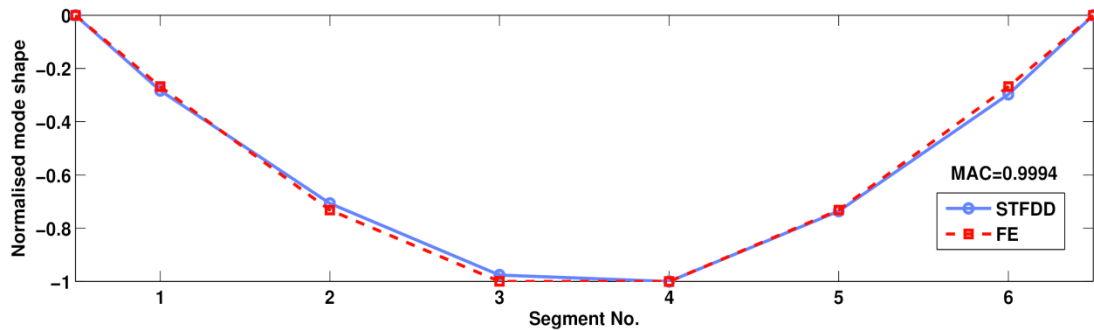
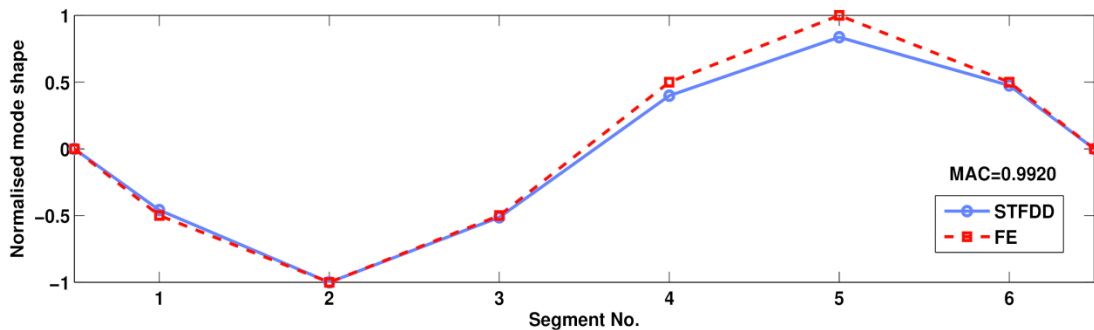


Figure 10: The SVD diagram obtained from Stage 3.



(a)



(b)

Figure 11: The first two mode shapes of the bridge (a) First mode shape, (b) Second mode shape.

5. Truck-trailers passing over a bridge with a Class A profile

A more general case of a truck with trailers is investigated in this section travelling over the same bridge as before with a Class A profile. The truck is heavy and used to excite the bridge. It is assumed to be towing two identical trailers, as illustrated in Fig. 12, and travelling at 1 m/s.

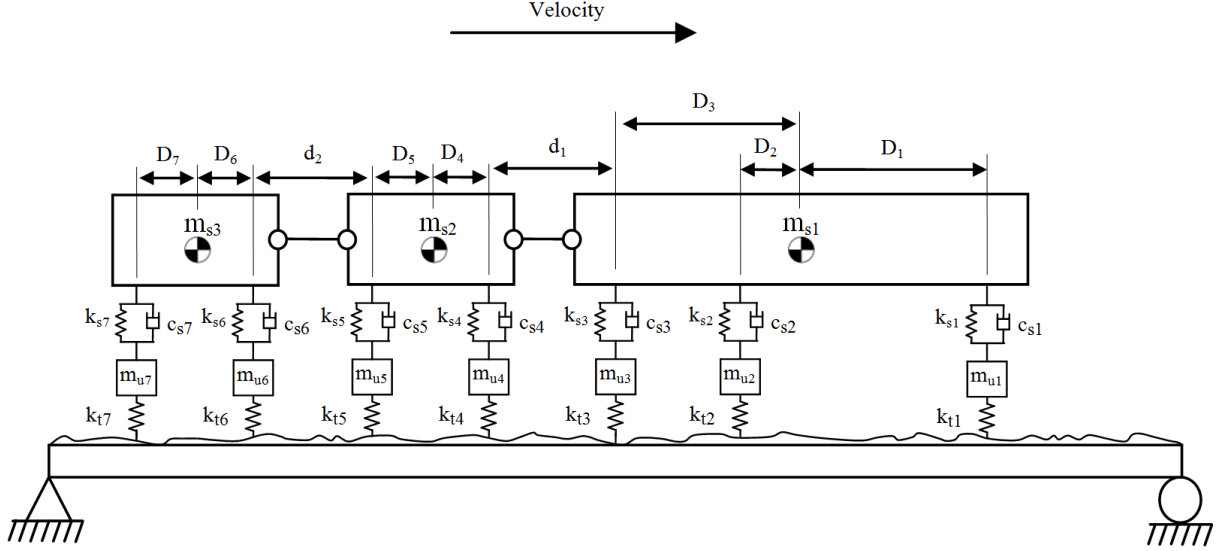


Figure 12: The truck-trailers model.

O'Brien et al. [43] give details of truck-trailer modelling in MATLAB. The properties of the truck and trailers are given in Tables 4 and 5 respectively. The same procedure of vehicle bridge interaction modelling which was used in previous sections is used in this case. The acceleration responses of Axles 4 through 7 are assumed to be measured. To remove the effect of road profile from the measured signals, two difference signals are defined as $\ddot{x}_1 = \ddot{y}_6 - \ddot{y}_4$ and $\ddot{x}_2 = \ddot{y}_7 - \ddot{y}_5$. The STFDD method is applied to these difference responses through five stages and five SVD diagrams are obtained. The SVD diagram from Stage 3 is shown in Fig. 13 as an example. The first two natural frequencies of the bridge are clearly detectable from this diagram. The mode shapes shown in Fig. 14 give a very good match to the exact shapes.

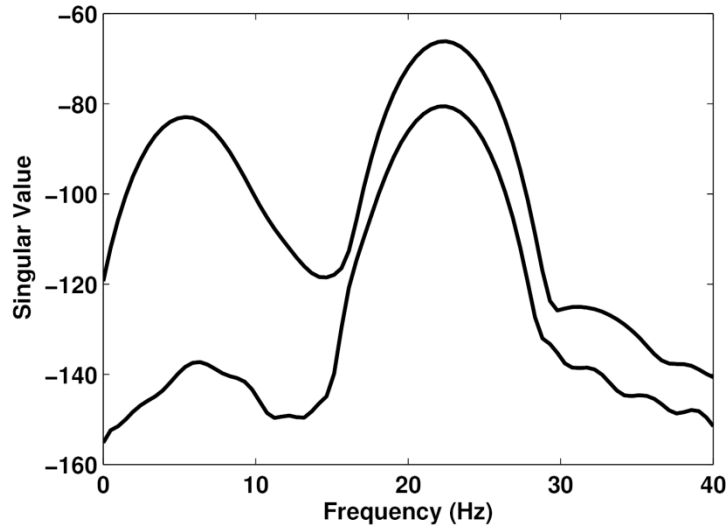


Figure 13: The SVD diagram obtained from Stage 3.

Table 4. Properties of the truck.

Property	Unit	Symbol	Value
Body mass	kg	m_{s1}	27100
Axle mass	kg	m_{u1}	700
		$m_{u2} = m_{u3}$	1100
Suspension stiffness	N/m	k_{s1}	4×10^5
		$k_{s2} = k_{s3}$	1×10^6
Suspension damping	Ns/m	c_{s1}	10×10^3
		$c_{s2} = c_{s3}$	20×10^3
Tyre stiffness	N/m	k_{t1}	1.75×10^6
		$k_{t2} = k_{t3}$	3.5×10^6
Moment of inertia	kg m ²	I_{s1}	1.56×10^5
Distance of axle to centre of gravity	m	D_1	4.57
		D_2	1.43
		D_3	3.23
Body mass frequency	Hz	$f_{body,1}$	1.32
Axle mass frequency	Hz	$f_{axle,1}$	8.82
		$f_{axle,2}$	10.17
		$f_{axle,3}$	10.20

Table 5. Properties of the trailers.

Property		Symbol	Value
Body mass	kg	m_{s2}	4000
Axle mass	kg	$m_{u4} = m_{u5} = m_{u6}$	50
Suspension stiffness	N/m	$k_{s4} = k_{s5} = k_{s6}$	4×10^5
Suspension damping	Ns/m	$c_{s4} = c_{s5} = c_{s6}$	10×10^3
Tyre stiffness	N/m	$k_{t4} = k_{t5} = k_{t6}$	1.75×10^6
Moment of inertia	kg m ²	I_{s2}	2401.67
Distance of axle to centre of gravity	m	$D_4 = D_5$	1.25
Body mass frequency	Hz	$f_{body,2}$	2.02
Axle mass frequency	Hz	$f_{axle,4}$	33.01
		$f_{axle,5}$	33.04
Distance of two trailers and truck to trailer	m	$d_1 = d_2$	1

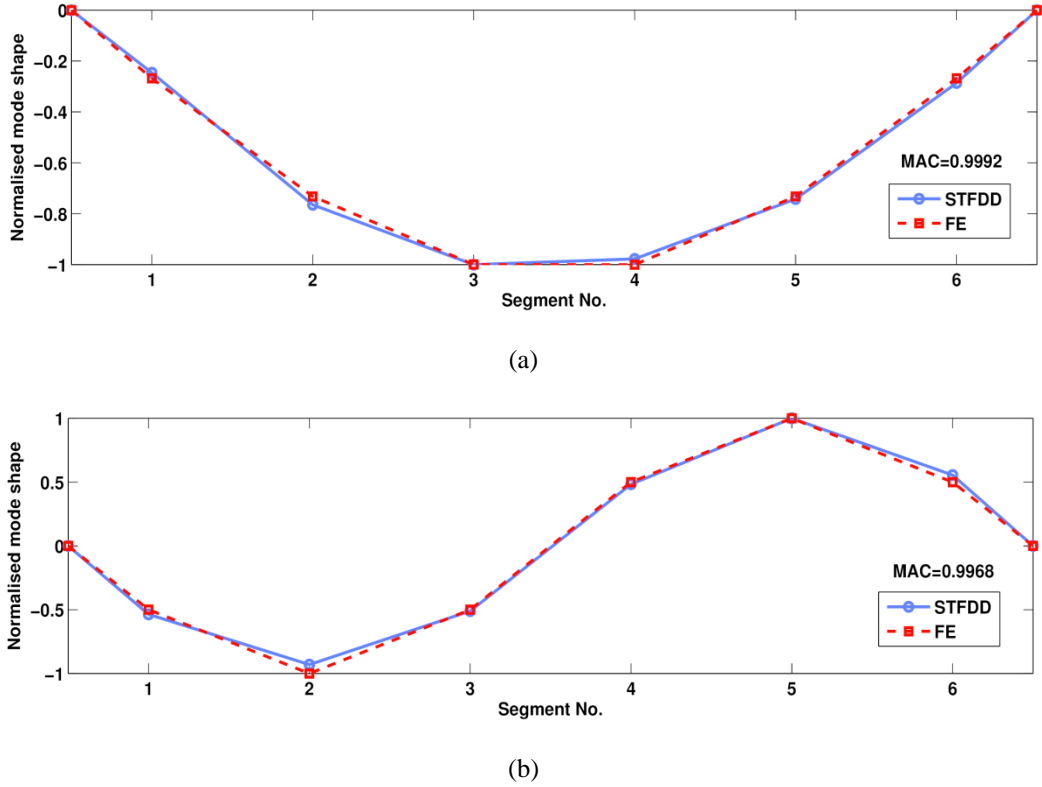


Figure 14: The first two mode shapes of the bridge. (a) First, (b) Second.

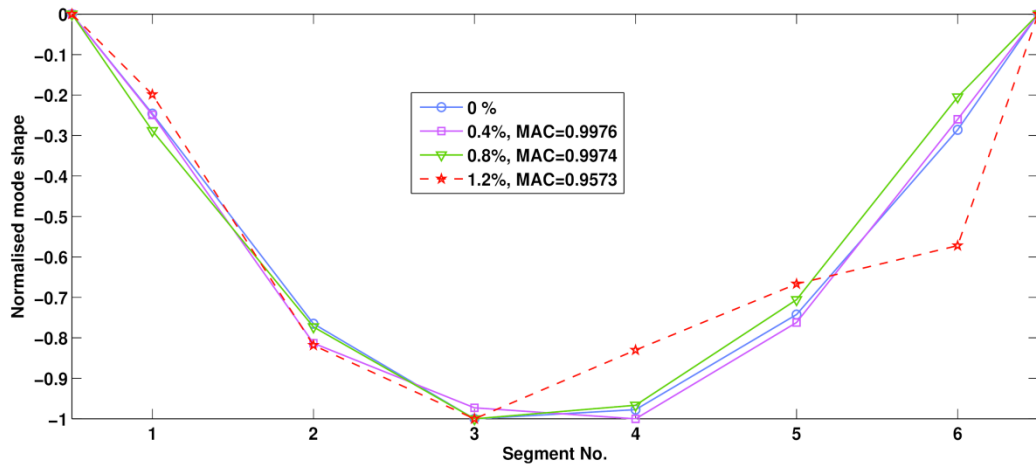
These calculated mode shapes are sensitive to noise, as can be seen in Fig. 15. The first mode is more sensitive than the second. In the opinion of the authors, this may be because the trailer body mass frequency is closer to the bridge first natural frequency than the second. Clearly, high-accuracy accelerometers will be needed to minimise measurement noise in the response.

6. Conclusion

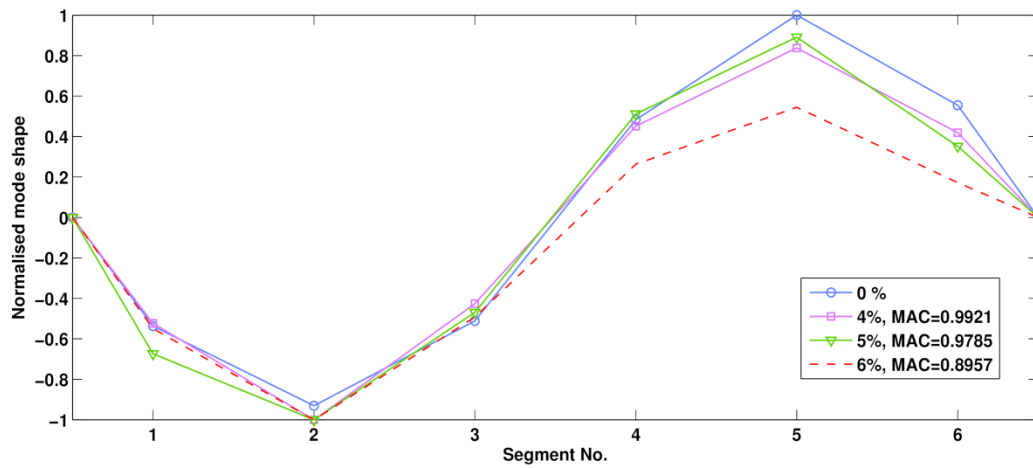
This paper describes a novel method for indirect identification of bridge mode shapes. When two following axles are modelled passing over a bridge, the FDD method can be applied to the short time measured signals obtained in several defined stages. By performing a rescaling procedure to the local mode shape vectors, the global mode shape is obtained. The performance of the proposed method is investigated using several numerical simulations. The effect of road profile in exciting the vehicle is a significant challenge for the method. Excitation of the bridge by other traffic improves the situation. In the absence of other traffic, subtraction of signals in identical axles is shown to be a feasible alternative. A truck towing two trailers is shown to be a possible arrangement for finding bridge mode shapes. Provided noise is sufficiently low, mode shapes can be found with good accuracy.

ACKNOWLEDGEMENTS

The authors wish to express their gratitude for the financial support received from Science Foundation Ireland towards this investigation under the US-Ireland Partnership Scheme.



(a)



(b)

Figure 15: Sensitivity of calculated mode shape vectors to noise; (a) first mode shape, (b) second mode shape.

References

- [1] Salawu OS. Detection of structural damage through changes in frequency: A review. *Engineering Structures*. 1997;19:718-23.
- [2] Kim JT, Stubbs N. Crack detection in beam-type structures using frequency data. *Journal of Sound and Vibration*. 2003;259:145-60.
- [3] Curadelli RO, Riera JD, Ambrosini D, Amani MG. Damage detection by means of structural damping identification. *Engineering Structures*. 2008;30:3497-504.
- [4] Williams C, Salawu OS. Damping as a damage indication parameter. 15th International Modal Analysis Conference. Orlando, FL, USA1997. p. 1531-6.
- [5] Kim JT, Ryu YS, Cho HM, Stubbs N. Damage identification in beam-type structures: frequency-based method vs mode-shape-based method. *Engineering Structures*. 2003;25:57-67.
- [6] Ewins DJ. *Modal testing : theory, practice, and application*. 2nd ed. Baldock, Hertfordshire, England: Research Studies Press Ltd.; 2000.

- [7] Carden EP, Fanning P. Vibration based condition monitoring: A review. *Struct Health Monit.* 2004;3:355-77.
- [8] Zhang L, Brincker R, Andersen P. An Overview of Operational Modal Analysis: Major Development and Issues. 1st IOMAC Conference. Copenhagen, Denmark 2005.
- [9] Ren WX, Peng XL, Lin YQ. Experimental and analytical studies on dynamic characteristics of a large span cable-stayed bridge. *Engineering Structures.* 2005;27:535-48.
- [10] Yang YB, Lin CW, Yau JD. Extracting bridge frequencies from the dynamic response of a passing vehicle. *Journal of Sound and Vibration.* 2004;272:471-93.
- [11] Yang YB, Lin CW. Vehicle-bridge interaction dynamics and potential applications. *Journal of Sound and Vibration.* 2005;284:205-26.
- [12] Lin CW, Yang YB. Use of a passing vehicle to scan the fundamental bridge frequencies: An experimental verification. *Engineering Structures.* 2005;27:1865-78.
- [13] Bu JQ, Law SS, Zhu XQ. Innovative bridge condition assessment from dynamic response of a passing vehicle. *J Eng Mech-Asce.* 2006;132:1372-9.
- [14] Yang YB, Chang KC. Extraction of bridge frequencies from the dynamic response of a passing vehicle enhanced by the EMD technique. *Journal of Sound and Vibration.* 2009;322:718-39.
- [15] Yang YB, Chang KC. Extracting the bridge frequencies indirectly from a passing vehicle: Parametric study. *Engineering Structures.* 2009;31:2448-59.
- [16] McGetrick PJ, Gonzalez A, OBrien EJ. Theoretical investigation of the use of a moving vehicle to identify bridge dynamic parameters. *Insight.* 2009;51:433-8.
- [17] Chang KC, Wu FB, Yang YB. Effect of road surface roughness on indirect approach for measuring bridge frequencies from a passing vehicle. *Interaction and multiscale mechanics.* 2010;3:299-308.
- [18] Kim CW, Isemoto R, Toshinami T, Kawatani M, McGetrick P, O'Brien EJ. Experimental Investigation of Drive-by Bridge Inspection. 5th International Conference on Structural Health Monitoring of Intelligent Infrastructure (SHMII-5). Cancun, Mexico 2011.
- [19] McGetrick P, Kim CW, O'Brien EJ. Experimental Investigation of the Detection of Bridge Dynamic Parameters Using a Moving Vehicle. The Twenty-Third KCCNN Symposium on Civil Engineering. Taipei, Taiwan 2010.
- [20] Yang YB, Li YC, Chang KC. Using two connected vehicles to measure the frequencies of bridges with rough surface: a theoretical study. *Acta Mech.* 2012;223:1851-61.
- [21] Gonzalez A, OBrien EJ, McGetrick PJ. Identification of damping in a bridge using a moving instrumented vehicle. *Journal of Sound and Vibration.* 2012;331:4115-31.
- [22] Yang YB, Chang KC, Li YC. Filtering techniques for extracting bridge frequencies from a test vehicle moving over the bridge. *Engineering Structures.* 2013;48:353-62.
- [23] Yang YB, Chen WF, Yu HW, Chan CS. Experimental study of a hand-drawn cart for measuring the bridge frequencies. *Engineering Structures.* 2013;57:222-31.
- [24] Keenahan J, OBrien EJ, McGetrick PJ, Gonzalez A. The use of a dynamic truck-trailer drive-by system to monitor bridge damping. *Struct Health Monit.* 2014;13:143-57.
- [25] Zhang Y, Wang LQ, Xiang ZH. Damage detection by mode shape squares extracted from a passing vehicle. *Journal of Sound and Vibration.* 2012;331:291-307.
- [26] Zhang Y, Lie ST, Xiang ZH. Damage detection method based on operating deflection shape curvature extracted from dynamic response of a passing vehicle. *Mech Syst Signal Pr.* 2013;35:238-54.
- [27] Li WM, Jiang ZH, Wang TL, Zhu HP. Optimization method based on Generalized Pattern Search Algorithm to identify bridge parameters indirectly by a passing vehicle. *Journal of Sound and Vibration.* 2014;333:364-80.

- [28] Yang YB, Li YC, Chang K. Constructing the mode shapes of a bridge from a passing vehicles: a theoretical study. *Smart Structures and Systems*. 2014;13:797-819.
- [29] Zhu XQ, Law SS. Wavelet-based crack identification of bridge beam from operational deflection time history. *Int J Solids Struct*. 2006;43:2299-317.
- [30] Pandey AK, Biswas M, Samman MM. Damage Detection from Changes in Curvature Mode Shapes. *Journal of Sound and Vibration*. 1991;145:321-32.
- [31] Arora V, Singh SP, Kundra TK. Damped model updating using complex updating parameters. *Journal of Sound and Vibration*. 2009;320:438-51.
- [32] Brincker R, Zhang LM, Anderson P. Modal identification from ambient response using frequency domain decomposition. *Proceedings of the 18th IMAC*. San Antonio, TX, USA2000.
- [33] Tan GH, Brameld GH, Thambiratnam DP. Development of an analytical model for treating bridge-vehicle interaction. *Engineering Structures*. 1998;20:54-61.
- [34] Kim CW, Kawatani M, Kim KB. Three-dimensional dynamic analysis for bridge-vehicle interaction with roadway roughness. *Comput Struct*. 2005;83:1627-45.
- [35] Harris NK, OBrien EJ, Gonzalez A. Reduction of bridge dynamic amplification through adjustment of vehicle suspension damping. *Journal of Sound and Vibration*. 2007;302:471-85.
- [36] Cantero D, OBrien EJ, González A. Modelling the vehicle in vehicle-infrastructure dynamic interaction studies. *P I Mech Eng K-J Mul*. 2010;224:243-8.
- [37] González A. Vehicle-bridge dynamic interaction using finite element modelling. *Finite element analysis*. Croatia: Sciyo; 2010. p. 637–62.
- [38] Cebon D. *Handbook of Vehicle-Road Interaction*. Lisse: Swets and Zeitlinger Publishers; 1999.
- [39] Clough RW, Penzien J. *Dynamics of Structures*: McGraw-Hill; 1993.
- [40] Tedesco JW, McDougal WG, Ross CA. *Structural dynamics: theory and applications*. California, USA: Addison- Wesley Longman; 1999.
- [41] Brincker R, Zhang LM, Andersen P. Modal identification of output-only systems using frequency domain decomposition. *Smart Mater Struct*. 2001;10:441-5.
- [42] ISO 8608:1995, *Mechanical Vibration-road Surface Profiles-reporting of Measured Data*, International Standards Organisation. 1995.
- [43] OBrien EJ, McGetrick PJ, González A. A drive-by inspection system via vehicle moving force identification. *Smart Structures and Systems*. 2014;13:821-48.